Water Research 118 (2017) 104–113

Contents lists available at ScienceDirect

Water Research

journal homepage: www.elsevier.com/locate/watres

Interaction between bacterial cell membranes and nano-TiO_2 revealed by two-dimensional FTIR correlation spectroscopy using bacterial ghost as a model cell envelope

Guocheng Huang [a], Tsz Wai Ng [a], Taicheng An [b, **], Guiying Li [b], Bo Wang [a], Dan Wu [a], Ho Yin Yip [a], Huijun Zhao [c, d], Po Keung Wong [a, *]

[a] School of Life Sciences, The Chinese University of Hong Kong, Shatin, NT, Hong Kong, China
[b] Institute of Environmental Health and Pollution Control, School of Environmental Science and Engineering, Guangdong University of Technology, Guangzhou, 510006, China
[c] Centre for Clean Environment and Energy, Griffith Scholl of Environment, Griffith University, Queensland, 4222, Australia
[d] Laboratory of Nanomaterials and Nanostructures, Institute of Solid State Physics, Chinese Academy of Sciences, Hefei, 230031, Anhui, China

ARTICLE INFO

Article history:
Received 20 January 2017
Received in revised form
4 April 2017
Accepted 8 April 2017
Available online 10 April 2017

Keywords:
Titanium dioxide nanoparticles
Bacterial ghosts
Two-dimensional FTIR correlation
Nanoparticle-cell membrane interaction

ABSTRACT

The interaction between microorganisms and nanoparticles is a crucial step towards understanding the subsequent biological effect. In this study, the interaction between TiO_2 nanoparticles and bacterial cell membrane was investigated by Two-dimensional Correlation Fourier Transformation Infrared spectroscopy (2D-FTIR-COS) using bacterial ghosts (BGs), which are non-living bacterial cell envelopes devoid of cytoplasm. The synchronous map of 2D-FTIR-COS results indicated that the functionalities in proteins of BGs preferentially interacted with TiO_2 nanoparticles; whereas the interaction of TiO_2 nanoparticles with characteristic functionality in polysaccharides (C—OH) and phospholipids (P═O) were very weak or insensitive. This conclusion was further corroborated by settling of TiO_2 nanoparticles in the presence of pure protein, polysaccharide and phospholipid represented by bovine serum albumin (BSA), alginate and phosphatidylethanolamine (PE). Additionally, the asynchronous map of 2D-FTIR-COS indicated a sequential order of functionalities bonded to TiO_2 nanoparticles with the order of: COO^- > aromatic C═C stretching > N—H, amide II > C═O, ketone. These findings contribute to deeper understanding of the interaction between TiO_2 nanoparticles and bacterial cell membrane in aquatic systems.

1. Introduction

Titanium dioxides (TiO_2) nanoparticles is one of the most widely used nanomaterials, with applications as cosmetics (Auffan et al., 2010), sunscreens (Nohynek et al., 2007), food additives (Weir et al., 2012) and photocatalysts (Hoffmann et al., 1995). The annual production of TiO_2 nanoparticles is rapidly increasing and estimated to reach 2.5 million metric tons by 2025 (Menard et al., 2011). Due to the increased production and application of synthetic TiO_2 nanoparticles, their release into the environment is inevitable. However, information regarding the TiO_2 nanoparticles toxicity, transport and fate in both natural and engineered systems is still scarce. Based on the existing studies, it is proposed that the interaction between nanoparticles and the membranes of microorganisms can be a critical initial process that precedes the toxicity pathways as well as influences the environmental fate of nanoparticles (Chen and Bothun, 2014).

To date, most related investigation on the interaction between cells and nanoparticles were mainly focused on how water chemistry, such as pH and ionic strength, affect the interaction between cells and nanoparticles (French et al., 2009; Ma et al., 2015). For example, solution pH determines the surface charges (i.e. zeta potentials) of both cells and nanoparticles, and thus influences the electrostatic interaction profile between the two objects. It was observed in many studies that low pH enhanced this interaction due to the nanoparticles being more positively charged while cells remaining negatively charged (Khan et al., 2011; Schwegmann et al., 2013). Salt ions can compress the electro-double layer of nanoparticles and cells, thereby reducing or eliminating the

* Corresponding author.
** Corresponding author.
E-mail addresses: antc99@gdut.edu.cn (T. An), pkwong@cuhk.edu.hk (P.K. Wong).

http://dx.doi.org/10.1016/j.watres.2017.04.023
0043-1354/

electro-double layer interaction. As a consequence, the commonly attractive van der Waals force becomes dominated and results in enhancement of cell surface and nanoparticle interaction under high ionic strength in water (Mukherjee and Weaver, 2010; Li et al., 2011; Shih et al., 2012). These results could be well described by the Derjaguin-Landau-Verwey-Overbeek (DLVO) theory due to the fact that the sizes of both microorganism cells and nanoparticles aggregates are within the scale of colloids. More recently, more comprehensive studies on the interaction between cell surface and nanoparticle in the presence of natural organic matters (NOM) have been carried out to mimic natural water environment (Lin et al., 2012). It was pointed out that both the bulk and nanoparticle-bound NOM can inhibit the interaction between cells and nanoparticles due to the delivery of negative charge to the surface of TiO_2 nanoparticles by NOM.

Approaches to probe the nanoparticle-membrane interaction are quite diverse, including by atomic force microscopy (AFM) (Leroueil et al., 2007; Roiter et al., 2008), optical tweezers (Rusciano et al., 2009), and quartz crystal microbalance with dissipation monitoring (QCM-D) (Keller and Kasemo, 1998; Zhang and Yang, 2011). QCM-D is the most extensively used tool for nanoparticle-membrane interaction due to its ability to in situ detection of nanoparticles adsorption on model cell membranes at a sensitivity level as low as tens of nanograms (Chen and Bothun, 2014). However, these techniques cannot distinguish which constituents or functionality of cell membrane correspond to the interaction when a membrane with multiple constituents is applied. Therefore, the binding affinities of cell surface constituents or functional groups to nanoparticles are unexplored.

Fourier transform-infrared (FTIR) spectroscopy is a versatile technique that offers a comprehensive insight into the molecular structure of principle constituents in bacterial cell membranes, such as protein, polysaccharide and lipid (Mecozzi et al., 2009). Two-dimensional correlation spectra (2D-COS), developed by Noda (1993), can be applied to resolve the overlapped peaks by distributing the spectral intensity trends along a second dimension with the data set collected as a function of a perturbation (e.g. time, temperature, concentration, etc.) (Noda, 1993; Dluhy et al., 2006). More importantly, it can also provide the information about the relative direction and sequential orders of structural variations in response to the perturbation. Thus, 2D-COS has been successfully applied to explore the interaction processes of NOM and TiO_2 nanoparticles (Chen et al., 2014). To the best of our knowledge, there is no literature reporting the application of 2D-FTIR-COS in the investigation on the interaction between nanoparticles and biological relevant components.

So far, the molecular mechanisms of the interaction between the NPs and bacterial cell membrane remain unclear, particularly, information on adsorption affinities of individual molecular constituents and functional groups is lacking. One of the major challenges is that cell membrane is dynamic and heterogeneous comprising multiple components such as phospholipid, protein, and polysaccharide (Chen and Bothun, 2014) that can lead to a more elaborate analysis of the mechanisms involved. Another challenge is that live cells undergoing metabolic process would secrete soluble microbial product (SMP) into the reaction solution and undoubtedly affect the interaction profile between cell surface and nanoparticles (Ni et al., 2011). A strategy to carry out nanoparticle-membrane interaction studies is to employ model membrane systems based on the phospholipid bilayer backbone of the cell membrane such as lipid vesicles (Hou et al., 2012; Lesniak et al., 2013; Chen and Bothun, 2014). Such systems can be further elaborated on by introducing other relevant components (i.e. protein and polysaccharides) that will make them more resemble the structure of cell membrane. Nevertheless, the synthesis of multi-components membrane architectures requires complex procedures and studies employing model membranes with embedded constituents such as protein and polysaccharide is still lacking to completely explore the interaction mechanism.

Bacterial ghosts (BGs) have recently emerged as novel vaccine candidates owing to their properties of being non-living bacterial cell membrane structure (cell envelopes) devoid of cytoplasmic constituents, and maintaining the full cellular morphology and surface constituents of their living counterparts (Jalava et al., 2002; Kudela et al., 2010). Moreover, the BGs can be easily produced by genetic methods or chemical methods (Mayr et al., 2005; Amara et al., 2013b). Therefore, it will be advantageous to employ BGs to study the interaction mechanisms of nanoparticles and cell membrane.

The purpose of this study, therefore, is to investigate the interaction between TiO_2 nanoparticles and cell membrane, by 2D-FTIR-COS technique, with BG as a model system. The settling experiments of standard protein, polysaccharide and phospholipid with TiO_2 were carried out to further verify and support the results.

2. Material and methods

2.1. Cell cultures and TiO_2 nanoparticles

Escherichia coli (*E. coli*) K-12 was used as model bacterium in this study. The bacterial cells were cultured in 50 mL Nutrient Broth 'E' (Lancashire, UK) with agitation at 200 rpm for 16 h. The cultures were then washed twice with sterile saline solution (0.9% NaCl) and resuspended in 50 mL sterilized saline solution with a cell density of ~2×10^9 colony forming unit per milliliter (cfu/mL). Degussa TiO_2 (P25, German) was used as a model TiO_2 nanoparticles in this study. The crystalline structures of the TiO_2 nanoparticles were identified through X-ray diffraction (XRD) analysis (Fig. S1). Its crystal structure consists of 80% anatase and 20% rutile, with an average primary size of 20–30 nm as revealed by transmission electron microscopic (TEM) analysis (Fig. S2), which were consistent with the description of manufacturer and published literature (Chowdhury et al., 2011; Tong et al., 2013a). A stock solution containing 10 g/L P25 solutions was used to prepare different concentrations of TiO_2 solutions.

2.2. BGs preparation and characterizations

The BGs were prepared according to a chemical method named "sponge-like" protocol (Amara et al., 2013a, 2013b). This method based on using active chemical reagents in concentration between Minimum Inhibition Concentration (MIC) and Maximum Growth Concentration (MGC) for bacteria. The MIC and MGC of were determined according to a previous report (Andrews, 2001), and shown in Table S1. Four chemical reagents were used in this protocol and their applied concentrations are determined as 4 mg/mL for SDS, 0.02 M for NaOH, 1.05 μg/mL for $CaCO_3$ and 64 mM for H_2O_2. In brief, 50 mL of washed cells were incubated with SDS, $CaCO_3$ and NaOH for 1 h to produce micropores on the surface of bacteria cells. Then the mixtures were centrifuged at 4000 rpm (Hermle Z323, Germany) for 10 min to evacuate the cytoplasmic constituent. The cell pellets were then washed with sterilized saline solution and resuspended in H_2O_2 solution for 30 min to guarantee the degradation of the residual DNA. Finally, the cells were collected by centrifugation at 4000 rpm and resuspended in 60% ethanol to remove any soluble organic residual. Then BGs were harvested by centrifugation at 4000 rpm and resuspended in 50 mL ultrapure water.

Light microscopy, scanning electronic microscope (SEM) and atomic force microscope (AFM) were used to observe the BGs as

well as the normal bacterial cells. Detailed descriptions of these works can be found in the Supporting Information. The DNA in the BGs and normal bacterial cells were, respectively, extracted using a Takara MiniBEST DNA Extraction Kit. DNA agarose gel electrophoresis (AGE) was also performed with 0.6% agarose gel at 80 V for 45 min in TAE buffer (40 mM Tris-acetate/1 mM EDTA, pH = 8) to determine the existence of any residual DNA in the BGs. The concentrations of extracted DNA were determined via a Nanodrop spectrophotometry (Model 2000C, Thermo Scientific, Waltham, MA, USA).

2.3. Interaction of BGs with TiO_2 nanoparticles

The BGs suspension was diluted to a concentration equivalent to ~2×10^8 cfu/mL in all the experiments unless otherwise stated. A series of BGs suspensions containing different concentrations of TiO_2 nanoparticles ranging from 0 to 200 mg/L were prepared and the final solution pH was adjusted to circumneutral condition (~6.8) using 0.01 M HCl and 0.01 M NaOH, which is close to the isoelectric point (IEP) of the TiO_2 nanoparticles (Huang et al., 2015). This pH condition can minimize the long-range electrostatic interaction (non-molecular interaction) and was environmental relevant (Parikh and Chorover, 2006). Then the suspensions were under vigorous agitation of 200 rpm for 8 h at 25 °C under dark in an incubator. Finally, 20 mL of each suspensions was sampled and freeze-dried for the FTIR measurement.

2.4. Spectroscopic parameters

An FTS-4000 Varian Excalibur series FT-IR spectrometer with attenuated total reflection (ATR) (Varian, Palo Alto, CA) was used to collect the infrared spectra. A mixture of the freeze-dried samples and 100 mg of potassium bromide (KBr, IR grade) were ground, homogenized and pressed. The band from 4000 to 400 cm^{-1} were collected with an interval of 2 cm^{-1}, and the ordinate was express as absorbance. Each spectrum was an average of 256 scans with automatic baseline correction. The obtained spectra were then smoothed using OMNIC 8.0 software for the subsequent analysis. The spectra of amide I region (1700-1600 cm^{-1}) were further analyzed to extract information regarding changes of the protein secondary structures by deconvolved spectra. A detailed description of the procedure can be found in the Supporting Information.

To assess the secretion of soluble microbial product (SMP) from normal cells of *E. coli* K-12, which may influence the interaction profile between TiO_2 nanoparticles and cell membranes, suspensions with 50 mL 2×10^8 cfu/mL normal *E. coli* K-12 cells were prepared under dark in the absence and presence of 100 mg/L TiO_2 P25 and shaken at 25 °C. Three mL suspension was sampled and filtered through a 0.22 μm nylon membrane to remove cells or/and TiO_2 nanoparticles at different time intervals. Then the filtrate was analyzed with a fluorescence spectrophotometer (F-7000, Hitachi, Japan) in excitation-emission-matrix (EEM) mode. Fluorescence EEM is a powerful tool to characterize SMP based on well-established principles (Hudson et al., 2007). For comparison, the fluorescence EEM of the bulk solution of BGs in the absence and presence of TiO_2 nanoparticles were also monitored.

2.5. 2D-FTIR-COS analysis

In this study, the TiO_2 nanoparticles concentration was applied as an external perturbation, and a set of concentration-dependent FT-IR spectra was obtained. Before conducting 2D-FTIR-COS, each FTIR spectrum was baseline-corrected and smoothed using Savitzky-Golay method (Wang et al., 2012; Chen et al., 2014). The practical computation of 2D-FTIR-COS was performed using Matlab R2010a (Mathworks Inc., USA) (Noda, 1993; Chen et al., 2015). The synchronous correlation intensity can be constructed using the following equation:

$$\varphi(\upsilon_1, \upsilon_2) = \frac{1}{m-1} \sum_{j=1}^{m} I_j(\upsilon_1) I_j(\upsilon_2) \tag{1}$$

Asynchronous correlation can be calculated by

$$\phi(\upsilon_1, \upsilon_2) = \frac{1}{m-1} \sum_{j=1}^{m} I_j(\upsilon_1) \sum_{j=1}^{m} N_{jk} I_j(\upsilon_2) \tag{2}$$

Where m is the total number of the collected spectra, $I_j(\upsilon)$ represents the intensity of the jth spectrum collected at a specific band or wavenumber of υ (denoting with a subscript of "1" or "2"). The term N_{jk} corresponds to the jth column and the kth row element of the discrete Hilbert-Noda transform matrix, which is defined as:

$$N_{jk} = \begin{cases} 0 & \text{if } j = k \\ \dfrac{1}{\pi(k-j)} & \text{otherwise} \end{cases} \tag{3}$$

The sign of the synchronous peaks $\varphi(\upsilon_1, \upsilon_2)$ reflects simultaneous changes in intensities measured at υ_1 and υ_2 in response to perturbation (Dluhy et al., 2006). A positive sign, $\varphi(\upsilon_1, \upsilon_2) > 0$, indicates the intensities change in the same direction (either increase or decrease simultaneously), while the trend is reversed for $\varphi(\upsilon_1, \upsilon_2) < 0$. The sign of the asynchronous peak $\phi(\upsilon_1, \upsilon_2)$ reflects the sequential order of the intensity change measured at υ_1 and υ_2 in response to perturbation. If $\varphi(\upsilon_1, \upsilon_2)$ and $\phi(\upsilon_1, \upsilon_2)$ have the same sign, the intensity change at υ_1 occurs predominantly before υ_2 while the rule is reversed if $\varphi(\upsilon_1, \upsilon_2)$ and $\phi(\upsilon_1, \upsilon_2)$ have the opposite sign.

2.6. TiO_2 precipitation with standard protein, polysaccharide and phospholipid

To further verify the role of the key biomolecular constituents in cell membrane in the interaction with TiO_2 nanoparticles, a series of settling experiments were performed according to previous studies (Lin et al., 2012; Ma et al., 2015). Bovine serum albumin (BSA), sodium alginate and phosphatidylethanolamine (PE) were used as standard biomolecular constituents to represent protein, polysaccharide and phospholipid, respectively. The mixed suspensions of 100 mg/L TiO_2 nanoparticles and biomolecular constituents with concentrations ranging from 0 to 200 mg/L were prepared (pH = 6.8) and subjected to settling experiments for 11 h, and their individual suspensions were also conducted as control. At different settling time, 1 mL aliquot of the mixed and individual suspensions were taken from the top of the suspension and immediately transferred into cuvettes to measure absorbance at 660 nm (A_{660}). The settling curves were plotted using the ratio of absorbance at a given time point (A_t) to the initial absorbance (A_0) as coordinate and time as abscissa.

3. Results

3.1. BGs as model cell envelope

To examine whether normal cells will secrete any SMP into the bulk solution, fluorescence EEM was applied to show the spectra of SMP secreted by normal cells of *E. coli* K-12 cells in the absence and presence of TiO_2 nanoparticles (Fig. 1). The peaks at Ex/Em of 230/340 nm (peak T1) and 280/340 nm (peak T2) are reported to be associated with the tryptophan-like protein (Hudson et al., 2007),

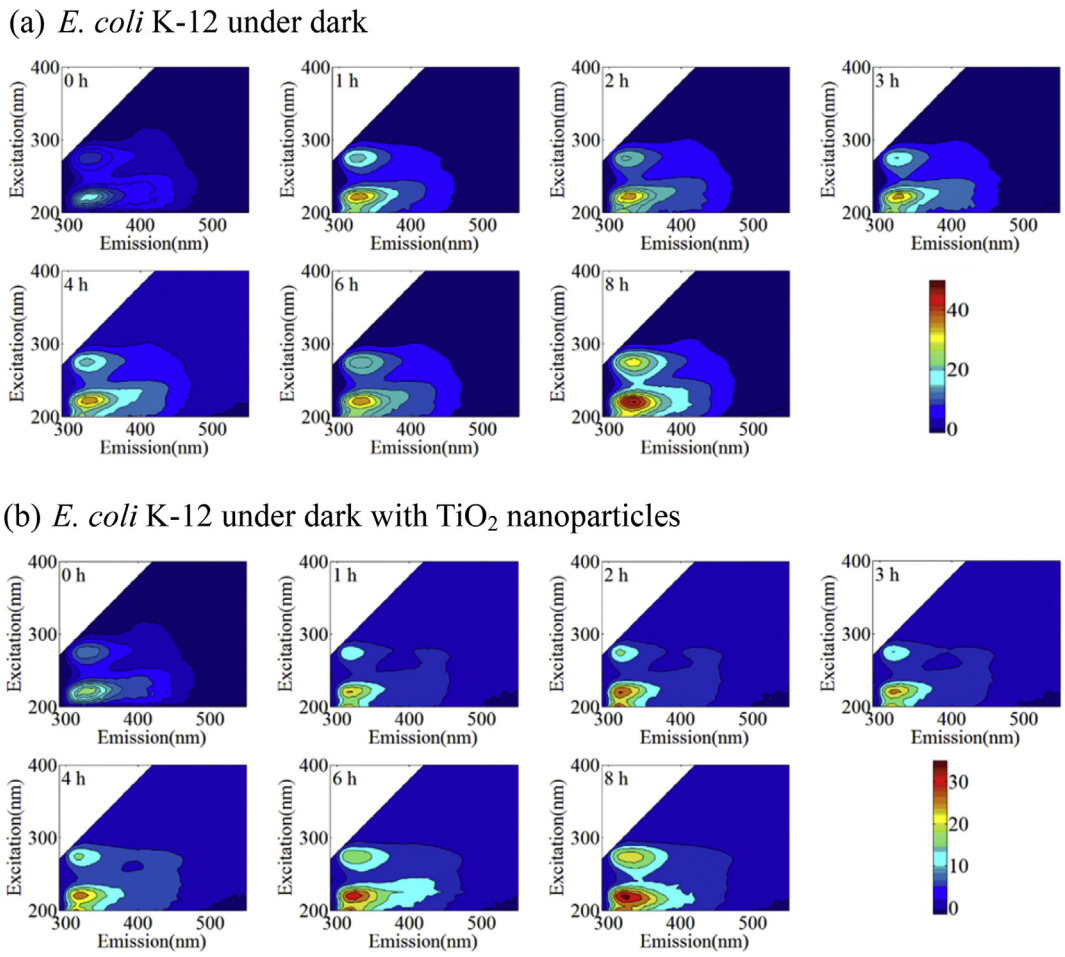

Fig. 1. Fluorescence contour plots of the SMP secreted by (a) *E. coli* cells under dark; (b) *E. coli* K-12 under dark with the presence of TiO_2 nanoparticles (100 mg/L).

which is a common fluorescent SMP secreted by bacterial cells. For *E. coli* cells under dark (Fig. 1a), the peak intensities increased along with time (Fig. S3a), suggesting that SMP was secreted into the bulk solution. With the addition of TiO_2 nanoparticles, the peak intensities still exhibited an increasing trend (Fig. 1b) along with time, while lower than those of sole *E. coli* cells at each time point (Fig. S3a). This difference was due to the released SMP adsorbing on the TiO_2 and thus led to a decrease of SMP concentration in the bulk solution. Therefore, the investigation of interaction between TiO_2 nanoparticles and cell membrane will certainly be affected by the presence of these release metabolic products. For example, it has been well-recognized that protein absorbed on nanoparticles surface to form nanoparticle-protein 'corona' (Mahon et al., 2012; Lesniak et al., 2013; Saptarshi et al., 2013), which would ultimately determine the interaction profile of nanoparticles with the biological membrane systems, rather than the pristine surface of the unmodified nanoparticles. For example, a previous study found that protein adsorption onto nanoparticles reduced their ability to adhere to cell surface (Lesniak et al., 2013). Therefore, employing model cell envelopes such as BGs, which lack metabolic activities, are of important merit to reveal an unbiased nanoparticle-membrane interaction mechanism.

To avoid the interference of SMP, BGs as model cell envelope was applied as model cell membrane in this study. Fig. 2 compares the SEM and AFM images of normal bacterial cell and BGs. The SEM and AFM images proved that the BGs were in good conditions and still maintained the 3D structure with micropores on the surface which were consistent with previous studies on the morphology of BGs (Amara et al., 2013b). Besides, the crystal violet stained BGs could be observed by light microscopy (Fig. S4), which was indicative of stable cell envelopes structure. Furthermore, the agarose gel electrophoresis results shown that no observable band on the lane of the BGs compared with the normal bacterial cells of *E. coli* K-12 (Fig. S5). The DNA concentrations for the BGs and normal bacterial cells were 1.7 ± 1.5 and 78.5 ± 1.3 ng/μL, respectively (Table S2). These results indicated the genomic DNA in the as-prepared BGs had been substantially degraded.

Additionally, the fluorescence EEM analysis of the bulk solution of BGs in the absence and presence of TiO_2 nanoparticles shown that fluorescence intensity at 230/340 and 280/340 nm were insignificant and remained constant along with time (Fig. S3b). This implied that the as-prepared BGs had lost metabolic activity and no SMP was produced due to the evacuation of the cytoplasmic constituents, which would allow us to avoid the interferences induced by the presence of SMP in the nanoparticles-membrane interaction studies.

3.2. 2D-FTIR-COS analysis on the interaction between TiO_2 nanoparticles and BGs

The FTIR spectra of the BGs as a function of TiO_2 nanoparticle concentrations are shown in Fig. S6. The spectral variations mainly occurred in the 1700–1000 cm^{-1} region, where the absorption changed significantly. An increase in TiO_2 nanoparticles

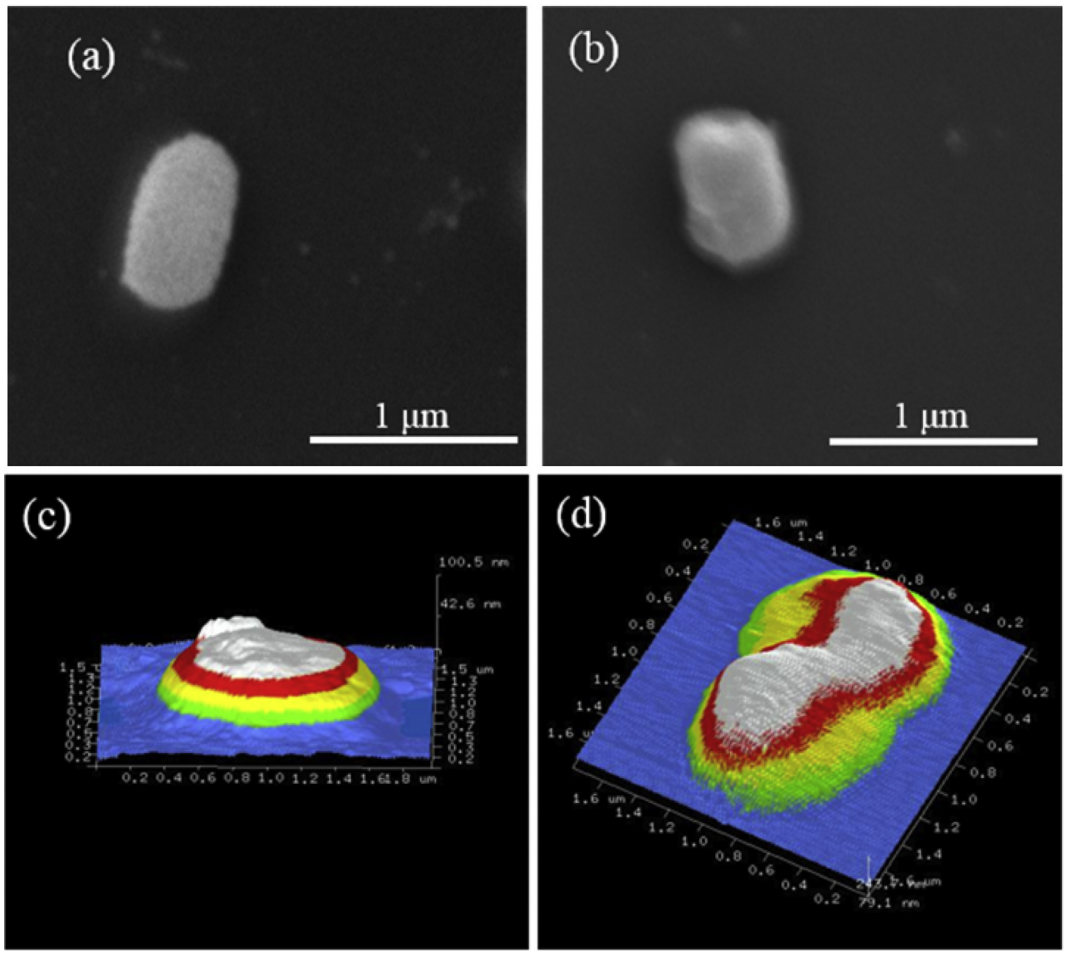

Fig. 2. SEM and AFM images of the normal *E. coli* K-12 cell (a, c) and bacterial ghost (b, d), respectively.

concentrations caused the characteristic bands changing to various degrees, indicating changes of vibrational structures in BGs by interacting with the TiO_2 nanoparticles. However, some of the bands strongly overlapped, and enhancement of the spectral resolution is needed to understand how individual IR band is subjected to the perturbation.

2D-FTIR-COS analysis can allow enhancing the spectral resolution by spreading overlap peaks in a second dimension, and as a result simplifying the interpretation of one dimension spectrum. Fig. 3 illustrates the synchronous and asynchronous FTIR maps of BGs with TiO_2 nanoparticles as the perturbation. The FTIR regions of bacteria, corresponding to the wavelength ranges of 1000–1200, 1200–1400, and 1500-1700 cm^{-1}, could be roughly assigned to polysaccharide, phospholipid, and protein, respectively (Schmitt and Flemming, 1998). Detailed spectral assignments are presented in Table 1. In synchronous maps (Fig. 3b) most autopeaks, which locate on the diagonal, appear in the protein region, suggesting that protein mainly responses to concentration perturbation. A prominent peak at 1000 cm^{-1} was due to the increased TiO_2 concentration (Fig. S7) (Kiwi and Nadtochenko, 2005). Therefore, the cross peaks located at 1000 cm^{-1} in the synchronous and asynchronous map will not be taken into consideration. Closer observation of the protein region (Fig. 3a) shows that all the cross peaks, which locate off the diagonal, exhibit positive signs, indicating that theirs intensity change in the same direction.

The asynchronous map can provide information on the sequential order of specific structural response to perturbation based on the signs of the cross peaks. In this study, red color indicates a positive sign, while blue color indicates a negative sign in the asynchronous map (Fig. 3c and d). Likewise, most of the cross peaks of the asynchronous map located in protein region (Fig. 3d). Specifically, four characteristic cross peaks were observed at the bands of 1612–1674, 1565–1612, 1550–1565 and 1400-1500 cm^{-1} (Fig. 3c), and the four bands were assigned to C=O stretching, COO^- symmetric stretching, N–H (amide II) and aromatic C=C stretching, respectively(Kiwi and Nadtochenko, 2005). The signs of the cross peaks (Table 1) indicate that sequential order of the bonding affinities of these bands with TiO_2 nanoparticles follow the order: COO^- → aromatic C=C stretching → N–H, amide II → C=O, ketone. It must be noted that the phospholipids and polysaccharides might also contain functional groups such as COO^-, C=O and aromatic C=C. However, in terms of their abundance in bacteria, the protein are rich in these functionalities, while the characteristic functional moieties for polysaccharide and phospholipid are C–O and P=O, which did not response to the perturbation. Results herein could roughly imply that the protein play a major role in the binding process of cell membrane to the TiO_2 nanoparticles.

3.3. Settling experiments

To further confirm the interpretation of the 2D-FTIR-COS results, a series of settling experiments were conducted using the selected protein, polysaccharide and lipid with TiO_2 nanoparticles. The

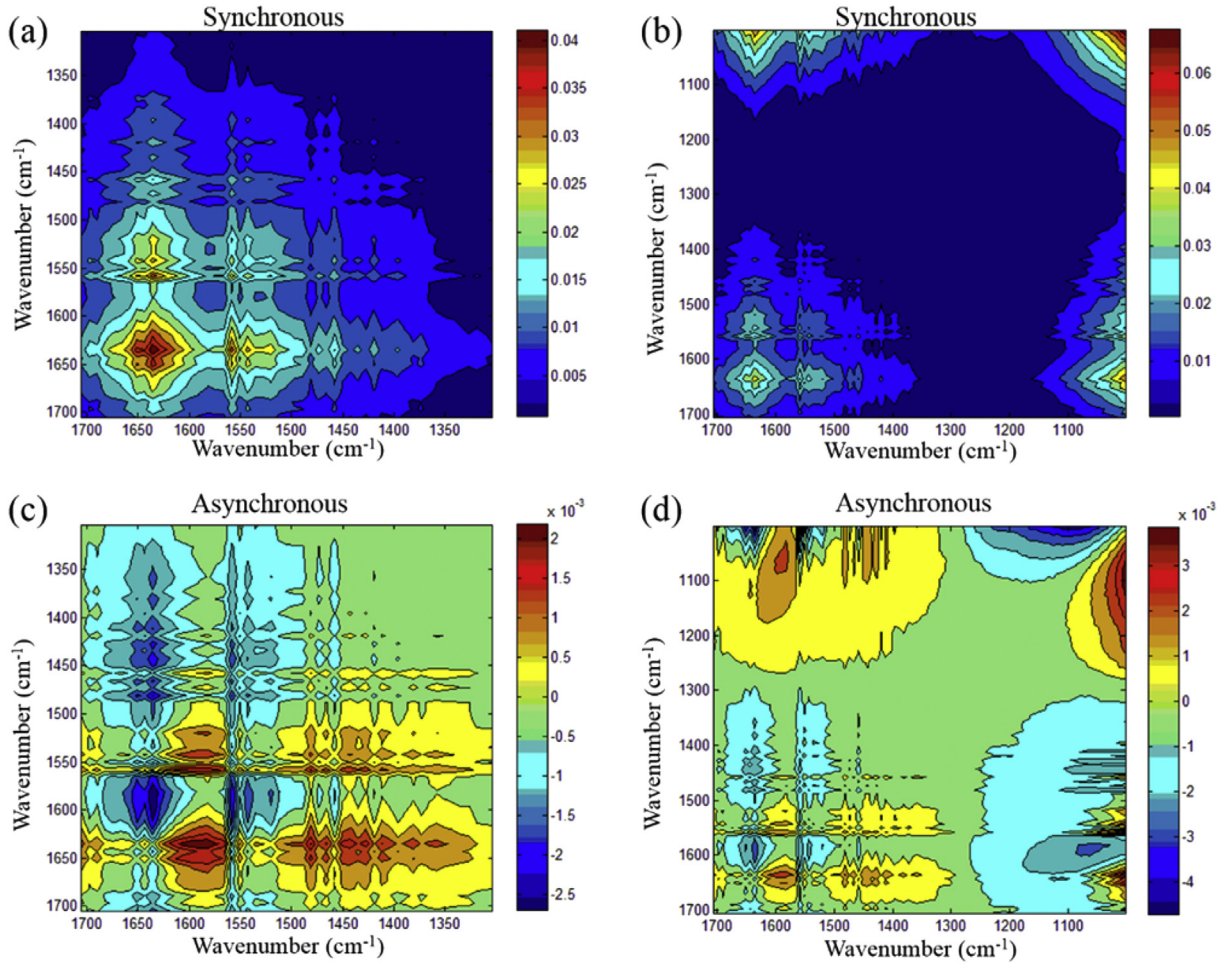

Fig. 3. Synchronous (a, b) and asynchronous (c, d) 2D-FTIR-COS maps generated from the 1700-1300 cm^{-1} region (a, c) and 1700-1000 cm^{-1} region (b, d) of the FTIR spectra of BGs with the increasing TiO_2 nanoparticles concentrations.

Table 1
2D-FTIR-COS result on the assignment and sign of each cross-peak in synchronous and asynchronous (in the brackets) map of BGs with increasing TiO_2 nanoparticle concentrations (Signs were obtained in the upper-left corner of the maps).

Region	Position (cm^{-1})	Possible assignment	Sign					
			Protein				Phosphate	Polysaccharide
			1612–1674	1565–1612	1550–1565	1400–1500	1200–1250	1100–1170
Protein	1612–1674	amide I, C=O stretching	+	+(−)	+(+)	+(−)	+(+)	+(+)
	1565–1612	aspartate or glutamate COO^- symmetric stretching		+	+(+)	+(+)	+(+)	+(+)
	1550–1565	amide II, N–H, C–N of protein			+	+(−)	+(+)	+(+)
	1400–1500	aromatic C=C stretching, C–H bend from CH_2				+	+(+)	+(+)
Phosphate	1200–1250	P=O from phosphate					0	+(0)
Polysaccharide	1100–1170	C–O stretching of polysaccharide						0

settling curves of the test substances at concentrations ranging from 0 to 200 mg/L with TiO_2 were shown in Fig. 4a, b and c. Significant biomolecule-type-dependent settlings were observed. Only protein mixed with TiO_2 shows precipitation behavior at concentrations higher than 10 mg/L, suggesting that protein interact with TiO_2 much stronger than polysaccharide and phospholipid. The photos of settling experiments of the three test substances at concentration of 100 mg/L are provided in Fig. 5. Additionally, comparison of the A_{660} (absorbance at 660 nm) value of the test substances before and after mixed with TiO_2 were also calculated by the following equation:

$$\Delta A = A_{\text{mixture}} - (A_{\text{test substance}} + A_{\text{TiO}_2}) \quad (4)$$

where A_{mixture} is the A_{660} of the mixture, and $A_{\text{test substance}}$, A_{TiO_2} represent the individual A_{660} of the test substances and TiO_2. In principle, a positive ΔA indicates interaction between TiO_2 nanoparticles and test substances as a result of forming test substances-TiO_2 hetero-agglomeration (Rieger et al., 2004; Lin et al., 2012). Conversely, zero or negative ΔA indicates no or very weak interaction between TiO_2 and the test substances. As shown in Fig. 4d, the ΔA had positive value at concentrations higher than 5 mg/L and exhibited an increasing trend with increasing concentrations,

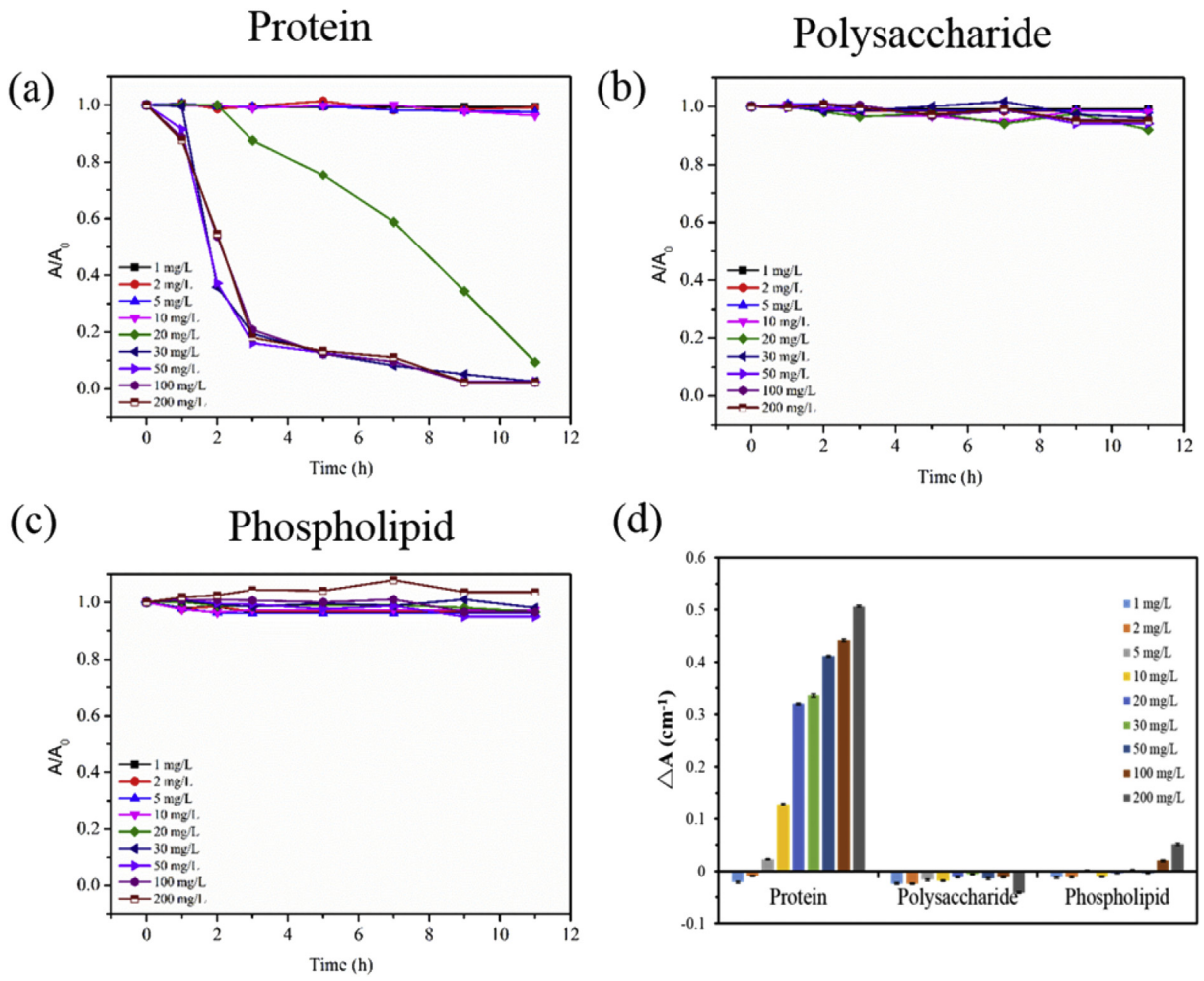

Fig. 4. (a) Settling curves of standard protein, (b) polysaccharide, (c) phospholipid with 100 mg/TiO_2 nanoparticles; and (d) the difference of absorbance at 660 nm of the test substances before and after mixed with TiO_2 nanoparticles.

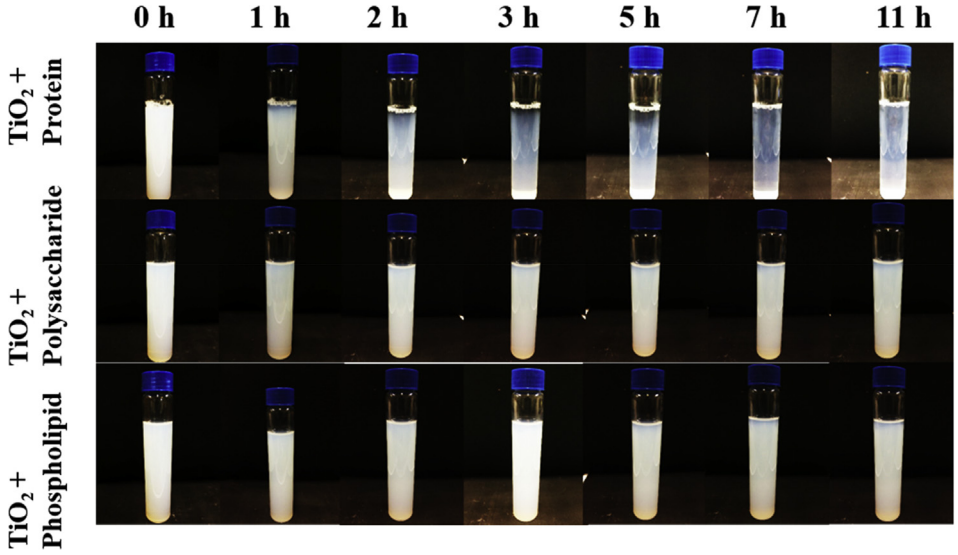

Fig. 5. Photos of the settling experiments of test substances with TiO_2 nanoparticle.

whereas no significant variations were observed with increasing polysaccharide and phospholipid concentrations mixed with TiO_2 nanoparticles. This suggests that TiO_2 nanoparticles preferentially interacted with protein and consequently formed larger hetero-agglomeration; while the interaction between TiO_2 nanoparticles and polysaccharide and phospholipid were weak or negligible.

Table 2
Band assignments for protein secondary structures of BGs and changes of the protein secondary structures exposed to increasing TiO_2 nanoparticles concentrations estimated by the curve fitting of the amide I region (1600 -1700 cm^{-1}) from the FT-IR spectra.

Secondary structures	Wavenumber (cm^{-1})	TiO_2 concentrations (mg/L)					
		0	25	50	100	150	200
Aggregated strands	1625–1610	5.25%	12.48%	12.36%	16.48%	16.60%	21.60%
β-Sheet	1640–1630	28.31%	24.53%	25.44%	30.72%	28.30%	19.79%
Unordered	1645–1640	–	14.99%	15.11%	15.34%	15.86%	19.50%
α-Helix	1657–1648	35.71%	17.61%	18.41%	15.65%	16.53%	18.11%
3-Turn helix	1666–1659	22.41%	19.36%	18.82%	15.00%	15.96%	16.56%
Antiparallel β-sheet/aggregated strands	1695–1680	8.32%	10.95%	9.82%	6.78%	6.72%	4.40%

4. Discussion

4.1. Increasing understanding of nanoparticle-cell membrane interaction

Understanding the interaction between nanoparticle and cell membrane is a crucial step toward predicting subsequent biological effects (Hou et al., 2012). As aforementioned, this interaction has been explored using various techniques and biological systems (e.g. cells and lipid bilayer) (Chen and Bothun, 2014). However, it is less clear what cell surface molecules are involved in the interaction (Chen and Bothun, 2014; Ma et al., 2015). This work for the first time specifically investigated the nanoparticle-cell membrane interaction using BGs as a model cell membranes at molecular level with 2D-FTIR-COS technique. The results of this study, revealed by the 2D-FTIR-COS, demonstrated that cell membrane functionalities of protein preferentially interacted with TiO_2 nanoparticle; whereas the interaction of TiO_2 nanoparticle with C—OH (polysaccharide) and P═O (phospholipid) were very weak or insensitive to IR. Although this adds to the limited literature regarding the roles of bacterial cell envelope biomolecules in the nanoparticle-membrane interaction, this finding is contradictory to previous reports. Jiang et al. (2010) previously reported that, in addition to protein, the lipopolysaccharide (LPS) also shown adhesive ability to metal oxides nanoparticles via hydrogen bonding with the O-antigen part (polysaccharide) using pure LPS extracted from *E. coli*. This discrepancy may have three possible explanations. First, the FTIR technique is insensitive to detect hydrogen bonding (Parikh and Chorover, 2006). Second, the level for LPS in *E. coli* K-12 bacterial cell envelope is much less than those for the phospholipid and protein, which are 4.73 and 4.83 times, respectively, higher than LPS level in terms molar ratio (Gmeiner and Schlecht, 1980). Third, the BGs maintain the phospholipid backbone structure with embedded protein, which may possibly compete with the LPS for absorption sites on the nanoparticles surfaces and thus leading to insignificant changes in the 2D-COS-FTIR response in the polysaccharide region. Whereas the study using extracted pure LPS only qualitatively represent the tendency of LPS to interact with nanoparticles regardless the three-dimensional structure of cell envelope. The current study cannot exclude the possibility of the interaction between LPS (polysaccharide) and TiO_2 nanoparticles when nanoparticles approach the bacterial surface. Nevertheless, our major findings herein indicate that protein plays dominant role in the interaction between TiO_2 nanoparticles and bacterial cell membrane. This was corroborated with the results from the settling experiments using standard protein, polysaccharide and phospholipid, which indicated the protein shown remarkable ability to form hetero-agglomeration with nanoparticles. Additionally, the asynchronous map of 2D-FTIR-COS indicates the propensities of functionalities bonded to TiO_2 nanoparticle followed as: COO^- > aromatic C═C stretching > N—H, amide II > C═O, ketone.

Knowledge on the interaction capacity and sequences of different biomolecules and functional groups of cell membrane to nanoparticles is supposed to bring new insight into the nanoparticle-membrane interactions and help to explain the toxicity of nanoparticles. For example, the nano-toxicity may possibly depend on the adhesion of nanoparticles on the cell membrane protein. Indeed, the cell membrane protein are suggested to be protected by the cell surface polysaccharide polymers and thus unlikely to interact with large particles. The interaction between the polysaccharide and large particle surface is unlikely to induce toxicity because this is similar to the manner in which bacteria adhere to large surfaces through the surface polymers in natural environment (Neu and Marshall, 1990). In contrast to their bulk counterparts, nanoparticles have extremely small sizes and therefore very likely to be able to travel across the gap between the surface polysaccharide polymers and reach the cell membrane surfaces. However, there exists consensus that nanoparticles with high surface energy typically tend to aggregate to form micro-scale agglomerates due to the unspecific interaction, thereby lowering their surface energy. Thus the interaction behavior between nanoparticles and cell membrane has been frequently elucidated as nanoparticles agglomerates with the cell membrane under static water condition and underlying mechanism could be interpreted by the DLVO theory which considers the sum of electrostatic and van der Waals interaction. This study conduct experiment under circumneutral condition which is close to the IEP of TiO_2 nanoparticles and thus tend to aggregate according to DLVO theory. In this case, there arises a concern that the results obtained from the micro-scale TiO_2 agglomerates did not realize the understanding in nano-scale. Nevertheless, it is important to note that the DLVO theory were based on the assumption of steady-state behavior of agglomerates and under static water conditions. We must recognize, however, that possible disruptions of aggregates due to the force induced by water flows (i.e. friction and lubrication or shear force) should be considered (Min et al., 2008; Nel et al., 2009). More importantly, natural and engineered aquatic systems typically under flowing condition. Therefore, the influence was environmental relevant and expected because of relative high agitation speed (200 rpm) were applied in this study. As a result, there should be likelihood of single nanoparticle or rafts from multiple particles directly bonding to the cell membrane surface protein due to their high propensity to interact with protein in the TiO_2-water-BGs system. This may lead to conformational changes of the protein and could be a possible reason for nanoparticle cytotoxicity. In this study, the changes in secondary structures of the protein in the BGs were characterized by the infrared self-deconvolution with second derivative resolution enhancement and with curve-fitting (Fig. S8). Results showed a decrease in α-helix contents and increase in the unordered and aggregate strands contents after exposed to nanoparticles (Table 2), indicating that the protein secondary structures were significantly changed and partial protein unfolding occurred after interacting with TiO_2 nanoparticles (Wu and Narsimhan, 2008). This is in accordance with the results of a previous study (Jiang et al., 2010), which also suggested that the protein damaged when exposed to TiO_2 nanoparticles and as a consequence leading

to loss physiological activities.

4.2. Significance for understanding the transport and fate of TiO_2 nanoparticles in natural system

In fact, apart from NOM and bacteria, protein are ubiquitously present in aquatic environments, particularly in wastewater-impacted water, as a result from microbial metabolism or anthropogenic input (Hudson et al., 2007; Meng et al., 2013). TiO_2 nanoparticles is increasingly being used in commercial products and it will be inevitably released into aquatic environments. Therefore, TiO_2 will finally meet NOM, bacteria and protein, which are likely to influence their transport. A previous study observed significant change in the aggregation state and deposition of TiO_2 nanoparticles in the presence of bacterial cells or/and NOM due to the changes of surface properties (Chowdhury et al., 2012). Nevertheless, how the protein affect the transport and fate of TiO_2 nanoparticles has seldom been considered. Our results herein suggested that the protein of the cell envelope or in the bulk solution play a critical role in the interaction with TiO_2 nanoparticles. Thus, the actual transport and fate of TiO_2 nanoparticles could be altered because the strong binding role of protein, considering the ubiquitousness of soluble protein in aquatic systems, especially in the anthropogenic-impact urban river with high SMP input from the waste water treatment plants (WWTPs) effluent.

4.3. Implications for the transport and fate of TiO_2 nanoparticles in engineered system

As the products of human activity, commercial TiO_2 nanoparticles have a high likelihood of entering municipal sewage that flows to centralized WWTPs, in which biological treatments were typically applied. It is very plausible that the majority of TiO_2 nanoparticles will be attached to the cell surface proteins of the activated sludge (mainly microorganisms) therein and their fate will be accompanied with the activated sludge. Given that the activated sludge could end up being as agricultural land amendments (fertilizers), placed in landfills, incinerated, or dumped into oceans (Kiser et al., 2009), the subsequent ecological impact and relative risk assessment remain unexplored and should be taken into consideration and examined in the future. In addition, the high propensity of proteins or COO^--rich substances to interact with TiO_2 nanoparticles provides a plausible clue for their removal in industrial wastewater where tremendous amount of TiO_2 nanoparticles waste are produced. Microorganisms/protein or COO^--rich substances could act as coagulant to remove TiO_2 nanoparticles wastes by sequential treatments of coagulation, flocculation and sedimentation (Serrao Sousa et al., 2017).

4.4. Technological aspects

The elucidation of nanoparticle-membrane interaction is beneficial for the design of novel nanoparticles which can work effectively in the presence of bacteria in water and wastewater treatment. Furthermore, the nanoparticle properties (i.e. sizes and shapes) will also influence the nanoparticle-cell membrane interaction (Tong et al., 2013b; Lin et al., 2014); thus more types of TiO_2 nanoparticles with different sizes and morphologies (i.e. nanotubes, nanorods and nanosheet, etc.) should be examined in the future. On the other hand, variation in bacterial cell envelope structure profiles (i.e. lipids with different tail length or degree of saturation, the levels of outer membrane protein, and lipopolysaccharide, etc.) could be manipulated via genetic approaches using relative mutants (Gao et al., 2012; Huang et al., 2015). BGs derived from the cell envelope-related mutants will enable one to determine the role of the interested gene products in the interaction between cell membrane and nanoparticles. Additionally, as membrane construction of Gram-positive and the Gram-negative bacteria are different, further studies using the BGs derived from Gram-positive bacteria (Abrams and Mcnamara, 1962) are therefore warranted. In general, the approach using BGs as model cell membrane combined with the 2D-FTIR-COS technique would provide an ideal platform to reveal the bionano surface interaction mechanism at molecular level.

5. Conclusions

The interaction between TiO_2 nanoparticles and bacterial cell membrane was investigated at molecular level using 2D-FTIR-COS analysis and BGs as model cell envelope. The main conclusions are:

- The synchronous map of 2D-FTIR-COS results shown that the functionalities in proteins of BGs have high propensity to interacted with TiO_2 nanoparticles, whereas the interaction of TiO2 nanoparticles with polysaccharides (C—OH) and phospholipids (P═O) were not detected under the test condition.
- The asynchronous map of 2D-FTIR-COS suggested a sequential order of functionalities bonded to TiO_2 nanoparticles with the order from high to low: COO^- > aromatic C═C stretching > N—H, amide II > C═O, ketone. These findings highlighted the role of protein in the interaction mechanisms between nanoparticles and bacterial cell membrane.
- Co-settling of TiO_2 nanoparticles with pure biomolecules (i.e., protein, polysaccharide and phospholipid) also highlighted the high propensity of protein molecules to interact with TiO_2 nanoparticles.
- 2D-FTIR-COS analysis using BGs as model cell membrane were shown to be a promising approach to investigating the molecular mechanisms by which nanoparticles interacting with bacterial cell membrane.
- This study could enhance our current knowledge on interaction mechanism of TiO_2 nanoparticles with bacterial cell membrane in water and has important implication for the nanotoxicity as well as the transport and fate of TiO_2 nanoparticles in the natural and engineered systems.

Acknowledgments

The project was supported by a research grant (GRF14100115) of the Research Grant Council, Hong Kong SAR Government. The project was also support by a Direct Grant from the Research Committee and a Technology and Business Development Fund (TBF15SCI008) from the Office of Research and Knowledge Transfer Services of The Chinese University of Hong Kong, and the research grant (41573086 and 41425015) of National Science Foundation of China to G.Y. Li and T.C. An. H.J. Zhao and P.K. Wong was also supported by CAS/SAFEA International Partnership Program for Creative Research Teams.

Appendix A. Supplementary data

Supplementary data related to this article can be found at http://dx.doi.org/10.1016/j.watres.2017.04.023.

References

Abrams, A., Mcnamara, P., 1962. Polynucleotide phosphorylase in isolated bacterial cell membranes. J. Biol. Chem. 237 (1), 170–175.

Amara, A.A., Salem-Bekhit, M.M., Alanazi, F.K., 2013a. Preparation of bacterial ghosts for *E. coli* JM109 using sponge-like reduced protocol. Asian J. Biol. Sci. 6, 363–369.

Amara, A.A., Salem-Bekhit, M.M., Alanazi, F.K., 2013b. Sponge-like: a new protocol for preparing bacterial ghosts. Sci. World J. 2013, 545741.

Andrews, J.M., 2001. Determination of minimum inhibitory concentrations. J. Antimicrob. Chemother. 48, 5–16.

Auffan, M., Pedeutour, M., Rose, J., Masion, A., Ziarelli, F., Borschneck, D., Chaneac, C., Botta, C., Chaurand, P., Labille, J., Bottero, J.Y., 2010. Structural degradation at the surface of a TiO_2-based nanomaterial used in cosmetics. Environ. Sci. Technol. 44 (7), 2689–2694.

Chen, K.L., Bothun, G.D., 2014. Nanoparticles meet cell membranes: probing nonspecific interactions using model membranes. Environ. Sci. Technol. 48 (2), 873–880.

Chen, W., Habibul, N., Liu, X.Y., Sheng, G.P., Yu, H.Q., 2015. FTIR and synchronous fluorescence heterospectral two-dimensional correlation analyses on the binding characteristics of copper onto dissolved organic matter. Environ. Sci. Technol. 49 (4), 2052–2058.

Chen, W., Qian, C., Liu, X.Y., Yu, H.Q., 2014. Two-dimensional correlation spectroscopic analysis on the interaction between humic acids and TiO_2 nanoparticles. Environ. Sci. Technol. 48 (19), 11119–11126.

Chowdhury, I., Hong, Y., Honda, R.J., Walker, S.L., 2011. Mechanisms of TiO_2 nanoparticle transport in porous media: role of solution chemistry, nanoparticle concentration, and flow rate. J. Colloid Interface Sci. 360 (2), 548–555.

Chowdhury, I., Cwiertny, D.M., Walker, S.L., 2012. Combined factors influencing the aggregation and deposition of nano-TiO_2 in the presence of humic acid and bacteria. Environ. Sci. Technol. 46 (13), 6968–6976.

Dluhy, R., Shanmukh, S., Morita, S.I., 2006. The application of two-dimensional correlation spectroscopy to surface and interfacial analysis. Surf. Interface Anal. 38 (11), 1481–1496.

French, R.A., Jacobson, A.R., Kim, B., Isley, S.L., Penn, R.L., Baveye, P.C., 2009. Influence of ionic strength, pH, and cation valence on aggregation kinetics of titanium dioxide nanoparticles. Environ. Sci. Technol. 43 (5), 1354–1359.

Gao, M., An, T., Li, G., Nie, X., Yip, H.Y., Zhao, H., Wong, P.K., 2012. Genetic studies of the role of fatty acid and coenzyme A in photocatalytic inactivation of Escherichia coli. Water Res. 46 (13), 3951–3957.

Gmeiner, J., Schlecht, S., 1980. Molecular composition of the outer-membrane of *Escherichia coli* and the importance of protein-lipopolysaccharide interactions. Arch. Microbiol. 127 (2), 81–86.

Hoffmann, M.R., Martin, S.T., Choi, W.Y., Bahnemann, D.W., 1995. Environmental applications of semiconductor photocatalysis. Chem. Rev. 95 (1), 69–96.

Hou, W.C., Moghadam, B.Y., Corredor, C., Westerhoff, P., Posner, J.D., 2012. Distribution of functionalized gold nanoparticles between water and lipid bilayers as model cell membranes. Environ. Sci. Technol. 46 (3), 1869–1876.

Huang, G.C., Xia, D.H., An, T.C., Ng, T.W., Yip, H.Y., Li, G.Y., Zhao, H.J., Wong, P.K., 2015. Dual roles of capsular extracellular polymeric substances in photocatalytic inactivation of *Escherichia coli*: comparison of *E. coli* BW25113 and isogenic mutants. Appl. Environ. Microbiol. 81 (15), 5174–5183.

Hudson, N., Baker, A., Reynolds, D., 2007. Fluorescence analysis of dissolved organic matter in natural, waste and polluted waters - a review. River Res. Appl. 23 (6), 631–649.

Jalava, K., Hensel, A., Szostak, M., Resch, S., Lubitz, W., 2002. Bacterial ghosts as vaccine candidates for veterinary applications. J. Control. Release 85 (1–3), 17–25.

Jiang, W., Yang, K., Vachet, R.W., Xing, B.S., 2010. Interaction between oxide nanoparticles and biomolecules of the bacterial cell envelope as examined by infrared spectroscopy. Langmuir 26 (23), 18071–18077.

Keller, C.A., Kasemo, B., 1998. Surface specific kinetics of lipid vesicle adsorption measured with a quartz crystal microbalance. Biophys. J. 75 (3), 1397–1402.

Khan, S.S., Srivatsan, P., Vaishnavi, N., Mukherjee, A., Chandrasekaran, N., 2011. Interaction of silver nanoparticles (SNPs) with bacterial extracellular proteins (ECPs) and its adsorption isotherms and kinetics. J. Hazard. Mater. 192 (1), 299–306.

Kiser, M.A., Westerhoff, P., Benn, T., Wang, Y., Perez-Rivera, J., Hristovski, K., 2009. Titanium nanomaterial removal and release from wastewater treatment plants. Environ. Sci. Technol. 43 (17), 6757–6763.

Kiwi, J., Nadtochenko, V., 2005. Evidence for the mechanism of photocatalytic degradation of the bacterial wall membrane at the TiO_2 interface by ATR-FTIR and laser kinetic spectroscopy. Langmuir 21 (10), 4631–4641.

Kudela, P., Koller, V.J., Lubitz, W., 2010. Bacterial ghosts (BGs)-Advanced antigen and drug delivery system. Vaccine 28 (36), 5760–5767.

Leroueil, P.R., Hong, S.Y., Mecke, A., Baker, J.R., Orr, B.G., Holl, M.M.B., 2007. Nanoparticle interaction with biological membranes: does nanotechnology present a janus face? Acc. Chem. Res. 40 (5), 335–342.

Lesniak, A., Salvati, A., Santos-Martinez, M.J., Radomski, M.W., Dawson, K.A., Aberg, C., 2013. Nanoparticle adhesion to the cell membrane and its effect on nanoparticle uptake efficiency. J. Am. Chem. Soc. 135 (4), 1438–1444.

Li, K.G., Zhang, W., Huang, Y., Chen, Y.S., 2011. Aggregation kinetics of CeO_2 nanoparticles in KCl and $CaCl_2$ solutions: measurements and modeling. J. Nanopart. Res. 13 (12), 6483–6491.

Lin, D.H., Ji, J., Long, Z.F., Yang, K., Wu, F.C., 2012. The influence of dissolved and surface-bound humic acid on the toxicity of TiO_2 nanoparticles to *Chlorella* sp. Water Res. 46 (14), 4477–4487.

Lin, X.C., Li, J.Y., Ma, S., Liu, G.S., Yang, K., Tong, M.P., Lin, D.H., 2014. Toxicity of TiO_2 nanoparticles to *Escherichia coli*: effects of particle size, crystal phase and water chemistry. PLoS One 9 (10).

Ma, S., Zhou, K.J., Yang, K., Lin, D.H., 2015. Heteroagglomeration of oxide nanoparticles with algal cells: effects of particle type, ionic strength and pH. Environ. Sci. Technol. 49 (2), 932–939.

Mahon, E., Salvati, A., Bombelli, F.B., Lynch, I., Dawson, K.A., 2012. Designing the nanoparticle-biomolecule interface for "targeting and therapeutic delivery". J. Control. Release 161 (2), 164–174.

Mayr, U.B., Walcher, P., Azimpour, C., Riedmann, E., Haller, C., Lubitz, W., 2005. Bacterial ghosts as antigen delivery vehicles. Adv. Drug Deliv. Rev. 57 (9), 1381–1391.

Mecozzi, M., Pietrantonio, E., Pietroletti, M., 2009. The roles of carbohydrates, proteins and lipids in the process of aggregation of natural marine organic matter investigated by means of 2D correlation spectroscopy applied to infrared spectra. Spectrochim. Acta Part A-Mol. Biomol. Spectrosc. 71 (5), 1877–1884.

Menard, A., Drobne, D., Jemec, A., 2011. Ecotoxicity of nanosized TiO_2. Review of in vivo data. Environ. Pollut. 159 (3), 677–684.

Meng, F.G., Huang, G.C., Yang, X., Li, Z.Q., Li, J., Cao, J., Wang, Z.G., Sun, L., 2013. Identifying the sources and fate of anthropogenically impacted dissolved organic matter (DOM) in urbanized rivers. Water Res. 47 (14), 5027–5039.

Min, Y.J., Akbulut, M., Kristiansen, K., Golan, Y., Israelachvili, J., 2008. The role of interparticle and external forces in nanoparticle assembly. Nat. Mater. 7 (7), 527–538.

Mukherjee, B., Weaver, J.W., 2010. Aggregation and charge behavior of metallic and nonmetallic nanoparticles in the presence of competing similarly-charged inorganic ions. Environ. Sci. Technol. 44 (9), 3332–3338.

Nel, A.E., Madler, L., Velegol, D., Xia, T., Hoek, E.M.V., Somasundaran, P., Klaessig, F., Castranova, V., Thompson, M., 2009. Understanding biophysicochemical interactions at the nano-bio interface. Nat. Mater. 8 (7), 543–557.

Neu, T.R., Marshall, K.C., 1990. Bacterial polymers: physicochemical aspects of their interactions at interfaces. J. Biomater. Appl. 5 (2), 107–133.

Ni, B.J., Rittmann, B.E., Yu, H.Q., 2011. Soluble microbial products and their implications in mixed culture biotechnology. Trends Biotechnol. 29 (9), 454–463.

Noda, I., 1993. Generalized two-dimensional correlation method applicable to infrared, Raman, and other types of spectroscopy. Appl. Spectrosc. 47 (9), 1329–1336.

Nohynek, G.J., Lademann, J., Ribaud, C., Roberts, M.S., 2007. Grey goo on the skin? Nanotechnology, cosmetic and sunscreen safety. Crit. Rev. Toxicol. 37 (3), 251–277.

Parikh, S.J., Chorover, J., 2006. ATR-FTIR spectroscopy reveals bond formation during bacterial adhesion to iron oxide. Langmuir 22 (20), 8492–8500.

Rieger, L., Langergraber, G., Thomann, M., Fleischmann, N., Siegrist, H., 2004. Spectral in-situ analysis of NO_2, NO_3, COD, DOC and TSS in the effluent of a WWTP. Water Sci. Technol. 50 (11), 143–152.

Roiter, Y., Ornatska, M., Rammohan, A.R., Balakrishnan, J., Heine, D.R., Minko, S., 2008. Interaction of nanoparticles with lipid membrane. Nano Lett. 8 (3), 941–944.

Rusciano, G., De Luca, A.C., Pesce, G., Sasso, A., 2009. On the interaction of nanosized organic carbon particles with model lipid membranes. Carbon 47 (13), 2950–2957.

Saptarshi, S.R., Duschl, A., Lopata, A.L., 2013. Interaction of nanoparticles with proteins: relation to bio-reactivity of the nanoparticle. J. Nanobiotechnol. 11.

Schmitt, J., Flemming, H.C., 1998. FTIR-spectroscopy in microbial and material analysis. Int. Biodeterior. Biodegrad. 41 (1), 1–11.

Schwegmann, H., Ruppert, J., Frimmel, F.H., 2013. Influence of the pH-value on the photocatalytic disinfection of bacteria with TiO_2 - explanation by DLVO and XDLVO theory. Water Res. 47 (4), 1503–1511.

Serrao Sousa, V., Corniciuc, C., Ribau Teixeira, M., 2017. The effect of TiO_2 nanoparticles removal on drinking water quality produced by conventional treatment C/F/S. Water Res. 109, 1–12.

Shih, Y.H., Zhuang, C.M., Peng, Y.H., Lin, C.H., Tseng, Y.M., 2012. The effect of inorganic ions on the aggregation kinetics of lab-made TiO_2 nanoparticles in water. Sci. Total Environ. 435, 446–452.

Tong, T.Z., Binh, C.T.T., Kelly, J.J., Gaillard, J.F., Gray, K.A., 2013a. Cytotoxicity of commercial nano-TiO_2 to *Escherichia coli* assessed by high-throughput screening: effects of environmental factors. Water Res. 47 (7), 2352–2362.

Tong, T.Z., Shereef, A., Wu, J.S., Binh, C.T.T., Kelly, J.J., Gaillard, J.F., Gray, K.A., 2013b. Effects of material morphology on the phototoxicity of nano-TiO_2 to bacteria. Environ. Sci. Technol. 47 (21), 12486–12495.

Wang, L.P., Shen, Q.R., Yu, G.H., Ran, W., Xu, Y.C., 2012. Fate of biopolymers during rapeseed meal and wheat bran composting as studied by two-dimensional correlation spectroscopy in combination with multiple fluorescence labeling techniques. Bioresour. Technol. 105, 88–94.

Weir, A., Westerhoff, P., Fabricius, L., Hristovski, K., von Goetz, N., 2012. Titanium dioxide nanoparticles in food and personal care products. Environ. Sci. Technol. 46 (4), 2242–2250.

Wu, X., Narsimhan, G., 2008. Characterization of secondary and tertiary conformational changes of beta-lactoglobulin adsorbed on silica nanoparticle surfaces. Langmuir 24 (9), 4989–4998.

Zhang, X.F., Yang, S.H., 2011. Nonspecific adsorption of charged quantum dots on supported zwitterionic lipid bilayers: real-time monitoring by quartz crystal microbalance with dissipation. Langmuir 27 (6), 2528–2535.